





Review: Revisiting the human cholinergic nucleus of the diagonal band of Broca

A. K. L. Liu*,¹ , E. J. Lim*,¹, I. Ahmed†, R. C.-C. Chang‡,§, R. K. B. Pearce* and S. M. Gentleman* 

*Neuropathology Unit, Division of Brain Sciences, Department of Medicine, Imperial College London, †Department of Eye Pathology, Institute of Ophthalmology, University College London, London, UK, ‡Laboratory of Neurodegenerative Diseases, LKS Faculty of Medicine, School of Biomedical Sciences and §State Key Laboratory of Brain and Cognitive Sciences, The University of Hong Kong, Pokfulam, Hong Kong

A. K. L. Liu, E. J. Lim, I. Ahmed, R. C.-C. Chang, R. K. B. Pearce, S. M. Gentleman (2018) *Neuropathology and Applied Neurobiology* 44, 647–662

Revisiting the human cholinergic nucleus of the diagonal band of Broca

Although the nucleus of the vertical limb of the diagonal band of Broca (nvIDBB) is the second largest cholinergic nucleus in the basal forebrain, after the nucleus basalis of Meynert, it has not generally been a focus for studies of neurodegenerative disorders. However, the nvIDBB has an important projection to the hippocampus and discrete lesions of the rostral basal forebrain have been shown to disrupt retrieval memory function, a major deficit seen in patients with Lewy body disorders. One reason for its neglect is that the anatomical boundaries of the nvIDBB are ill defined and this area of the brain is not part of routine diagnostic sampling protocols. We have reviewed the history and anatomy of the nvIDBB and now propose guidelines for distinguishing nvIDBB

from other neighbouring cholinergic cell groups for standardizing future clinicopathological work. Thorough review of the literature regarding neurodegenerative conditions reveals inconsistent results in terms of cholinergic neuronal loss within the nvIDBB. This is likely to be due to the use of variable neuronal inclusion criteria and omission of cholinergic immunohistochemical markers. Extrapolating from those studies showing a significant nvIDBB neuronal loss in Lewy body dementia, we propose an anatomical and functional connection between the cholinergic component of the nvIDBB (Ch2) and the CA2 subfield in the hippocampus which may be especially vulnerable in Lewy body disorders.

Keywords: Alzheimer's disease, basal forebrain, cholinergic system, diagonal band of Broca, Lewy body dementia, Parkinson's disease

Introduction

Brain cholinergic neurotransmitter systems are instrumental in many behavioural and cognitive processes including attention, learning, memory, arousal and sleep [1,2]. As suggested in the 'Cholinergic

hypothesis', a decreased level of acetylcholine in the cerebral cortex and hippocampus has been shown to contribute to the cognitive decline seen in ageing and Alzheimer's disease (AD) [3]. The cholinergic innervation of the neocortex and allocortex originates from the cholinergic basal forebrain complex. In humans, this complex is composed of interdigitating cell groups with approximately 200 000 neurons per hemisphere [4–6].

Using acetylcholinesterase (AChE) histochemistry and choline acetyltransferase (ChAT) immunohistochemistry, Mesulam and colleagues introduced 'Ch' sectoral terminology to distinguish four groups of ChAT-

Correspondence: Alan K. L. Liu, Division of Brain Sciences, Department of Medicine, Imperial College London, 4/F, Burlington Danes Building, Du Cane Road, London W12 0NN, UK. Tel: +44 (0)2075946586; E-mail: king.liu09@imperial.ac.uk

¹These authors contributed equally to this work.

immunopositive neurons within the basal forebrain based on morphology and rostral–caudal organization [7,8]. Ch1–Ch4 correspond to the cholinergic neurons found in the medial septal nucleus (MSN), the nucleus of the vertical limb of the diagonal band of Broca (nvIDBB), the nucleus of the horizontal limb of the DBB (nhIDBB) and the nucleus basalis of Meynert (nbM), respectively. Retrograde tracer experiments using horseradish peroxidase in nonhuman primates showed that Ch1 and Ch2 provide cholinergic efferents to the hippocampal complex, Ch3 to the olfactory bulb and Ch4 to the neocortex and amygdala.

With over 90% of its magnocellular neurons being cholinergic, the nbM is the largest and most well-studied cell group within the cholinergic basal forebrain. Degeneration of the nbM has been correlated with the presence of dementia in neurological conditions and we have previously hypothesized that subregions of the nbM are differentially affected in Parkinson's disease (PD) and AD [9]. By contrast, pathology within the nvIDBB, which is the second largest cholinergic group in the basal forebrain and with up to 70% of neurons being ChAT-positive, is much less well characterized in neurodegenerative conditions.

Given that hippocampal pathology is implicated in many dementing disorders and with the hippocampus receiving extensive innervation from the nvIDBB, it is important now to revisit this relatively neglected cholinergic cell group. Furthermore, there is a significant overlap between the nvIDBB and adjacent cholinergic loci, so there is as yet no clear consensus on its

anatomical boundaries. Here, on the basis of a review of the history and anatomy of the rostral basal forebrain, we provide recommendations for the visualization and sampling of the human nvIDBB. In addition, we have reviewed clinicopathological studies involving the nvIDBB and postulate a role for cholinergic inputs from this nucleus in the cognitive decline seen in PD and AD.

Historical perspectives

Coining the term diagonal band (of Broca)

In a series of monographs published in the 1870s and 1880s comparing the great limbic lobes (*Le grand lobe limbique*) in the brains of different mammalian species [10–12], French physician and anatomist Pierre Paul Broca defined a 'diagonal band' (*La bandelette diagonale*) within a quadrilateral space located directly superior to the optic chiasm (Figure 1). He described the band as seen from the inferior surface of the brain to run diagonally from the anterior and 'outermost' portion of the 'hippocampal lobe' to the root of the olfactory tract, joining the medial olfactory striae at the midline. On macrodissection, Broca related that the diagonal band passes in front of the optic chiasm and descends into the hemisphere. It then travels anterior to the anterior commissure and the medial septal fibres towards the genu of the corpus callosum. At a coronal level, this can be identified clearly as a white-matter bundle medial to the nucleus accumbens of the basal ganglia

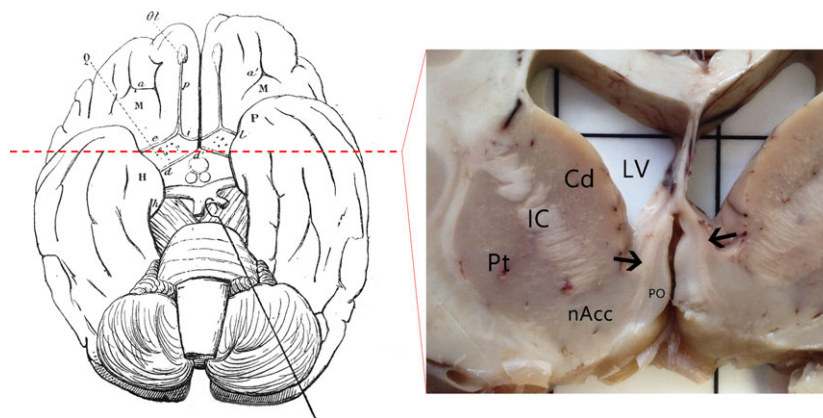


Figure 1. An illustration of the diagonal band (d–d') in the human brain seen from the inferior surface, with the optic tract retracted, as described in Broca's monograph in 1888 [12] (left). Coronal section at a level approximately 1.5 cm anterior to the mammillary bodies (red dashed line) revealed the extent of the diagonal band (black arrows) on both sides of the hemisphere, medial to the basal ganglia (right). Cd, caudate; IC, internal capsule; LV, lateral ventricle; nAcc, nucleus accumbens; PO, paraolfactory area; Pt, putamen.

(Figure 1). Further afield, the course of the diagonal band became difficult to follow, but Broca postulated that most of the fibres travel behind the corpus callosum and establish a direct connection between this lobe and the hippocampus. This projection is similar to the septal arcuate fibres described by Karl Friedrich Burdach in 1822 which is probably identical to the tract described by Broca [13]. Sir Grafton Elliot Smith, an Australian-British anatomist, acknowledged Broca's work and introduced the term DBB to the English literature [14].

Defining the 'nucleus' of the DBB

Previously mistaken as the medial paraolfactory nucleus, the nucleus of the DBB (nDBB) was first described in the brains of box turtles (*Cistudo Carolina*) as a cell mass extending from just rostral to the anterior commissure decussation down to the optic chiasm and caudal to the basolateral surface of the amygdaloid complex [15]. Subsequently, the nDBB was described in alligators (*Alligator mississippiensis*) [16], opossums (*Didelphis virginiana*) [17,18], rabbits [17] and rats [19]. The nDBB was also described in the brain of an 8-month-old human foetus in a comparative neuroanatomy study [17]. Johnson reported that the nDBB started at the lower border of the septum pellucidum bounded laterally by the olfactory tubercle. He then described magnocellular and 'deeply stained' cells of the diagonal band extending 'laterally close beneath the internal capsule to the temporal limb of the anterior commissure'. He also noticed a bundle or tract which runs among the diagonal band cells ventral to the basal ganglia and parallel to the basal surface of the brain, descending into the temporal pole with the anterior commissure at its caudal end. Based on his description, it is likely that he was describing the nbM and that the bundle he described was not the diagonal band but was rather the ansa lenticularis and ansa peduncularis. This highlights the differential organization and localization of basal forebrain cell groups in different animal species. A large mass of nDBB cells seen in most other mammalian species is replaced by an extensive nbM in human and other nonhuman primates. It was not until the 1930s when comparative neuroanatomical study was performed on the brains of rhesus monkeys by Papez and Aronson that the primate nDBB was more properly defined [20]. The

authors noted the important distinction that the nDBB is a 'distinct band of deeply staining cells' embedded within and following the course of the DBB.

Subdivisions and the two 'limbs' of the DBB

Building on Papez's study, Herald Brockhaus was first to extensively characterize the nDBB (*die kerngruppe des diagonalen Bandes*) in humans in his comparative study of the basal forebrain cell groups (*Basalkernkomplex*) in primates [21]. Based on the cell morphology, location and orientation, Brockhaus subdivided the nDBB rostrocaudally into the *nucleus diagonalis septalis*, *angularis* and *ventralis*. Subsequently, in a study of the septum in the human brain, Andy and Stephan divided the nDBB into 'tubercular' and 'septal' parts, with the septal part located against the medial septum, and the tubercular part located against the ventral aspect (olfactory tubercle) of the brain [22]. In both subdivision schemes, the borders between subdivisions were arbitrarily defined and lack any functional significance.

Experimental lesioning of the fimbria-fornix in rats, rabbits and the macaque monkey has demonstrated retrograde degeneration of the MSN and the nDBB, but limited to the vertical limb of the nucleus [23]. Subsequently, division of the nDBB into vertical and horizontal limbs has become well accepted due to their distinct delineation and anatomical connections. Their distinct anatomical efferents were confirmed by retrograde tracer experiments, demonstrating that nvDBB (along with MSN) projects to the hippocampal formation and nhlDBB projects to the olfactory bulb.

Anatomy of the nDBB

Extent of the diagonal band at different coronal levels

As described previously, the diagonal band emerges at the base of the brain and travels inward medially and rostrally to join the medial septal fibres by the genu of the corpus callosum. It is possible to map the extent of the diagonal band at several coronal levels rostrocaudally using established stereotaxic human brain atlases [24–26] (Figure 2).

At the rostral-most level (here we term the 'pre-commissural level' of the anterior basal ganglia due to the

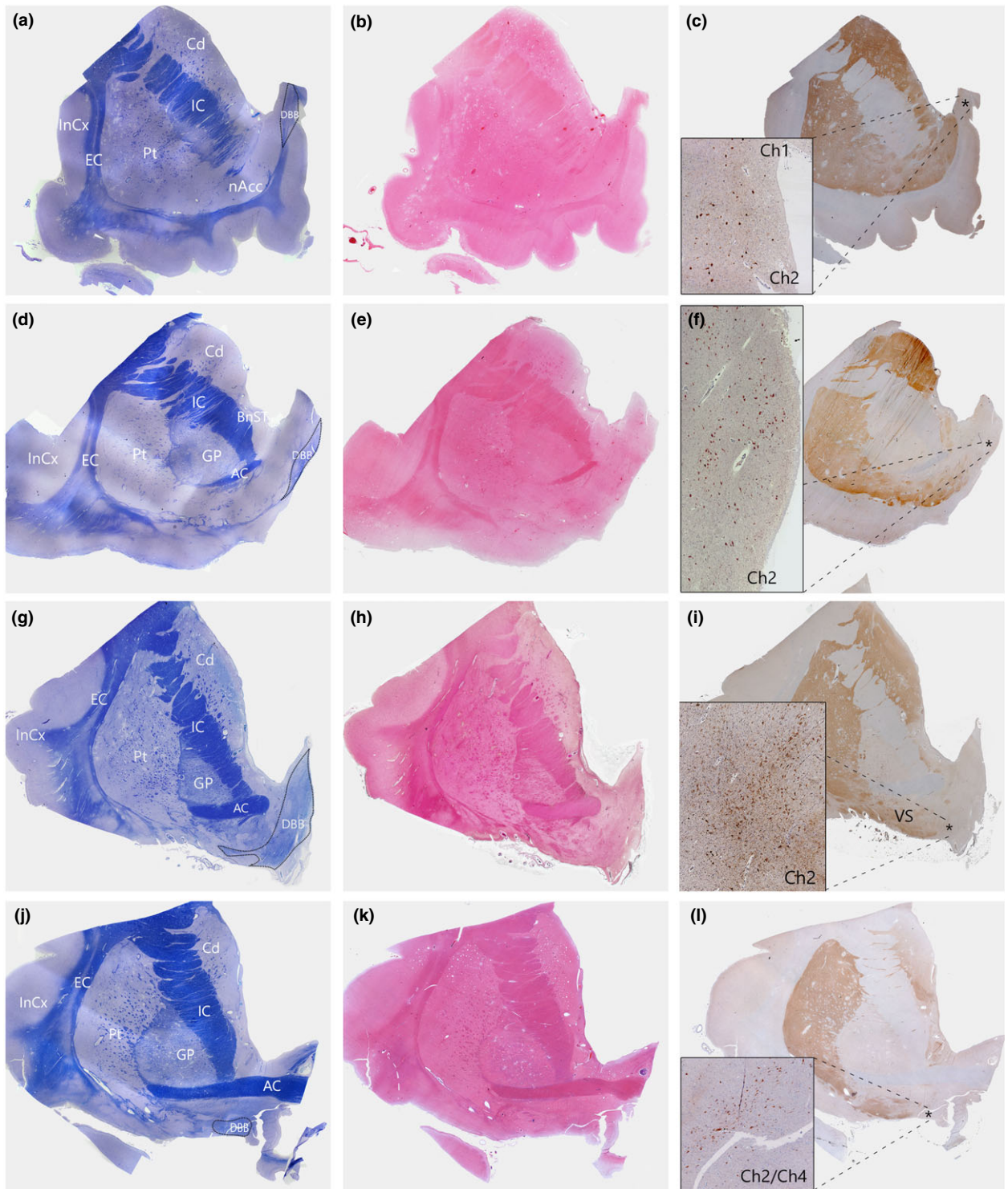


Figure 2. Serial sections of human basal forebrain tissues at different coronal levels were stained with cresyl violet and luxol fast blue (CV/LFB) for the visualization of neurons and fibre tracts (a,d,g,j); H&E for identification of anatomical landmarks (b,e,h,k); and immunostained for ChAT (Millipore AB144P, 1:100 with antigen-retrieval using pressure cooker pretreatment in pH6.0 citrate buffer) for the identification of the cholinergic population within the nvIDBB (c,f,i,l). The DBB was identified at four distinct levels, arranged rostrally (top) to caudally (bottom). (a–c) Precommissural level. At this level, the nucleus accumbens is prominent with the absence of anterior commissure fibre. The DBB can be seen at the medial and dorsal aspects, merging with the medial septum. Here, the Ch1 and Ch2 populations are often difficult to be distinguished. (d–f) Rostral predecussation level. The anterior commissure begins to emerge and the DBB is situated slightly more ventrally. ChAT-positive neurons within the nvIDBB increase in density. (g–i) Caudal predecussation level. At this level, the DBB sits at the ventromedial aspect of the basal forebrain and the Ch2 population reaches the maximum. (j–l) Anterior commissure decussation level. Here, the anterior commissure begins to decussate and the DBB is situated ventrally, parallel to the ventral border of the basal forebrain. ChAT-positive neurons of the nvIDBB intermingle with those in the nbM at this level. Asterisk (*) denotes area of maximum density of ChAT-positive neurons. BnST, bed nucleus of stria terminalis; Cd, caudate; ChAT, choline acetyltransferase; Ch1, cholinergic neurons in the medial septal nucleus; Ch2, cholinergic neurons in the vertical limb of the diagonal band of Broca; Ch4, cholinergic neurons in the nbM; nvIDBB, nucleus of the vertical limb of the DBB; EC, external capsule; GP, globus pallidus; IC, internal capsule; InCx, insular cortex; nAcc, nucleus accumbens; Pt, putamen; VS, ventral striatum; nbM, Nucleus basalis of Meynert.

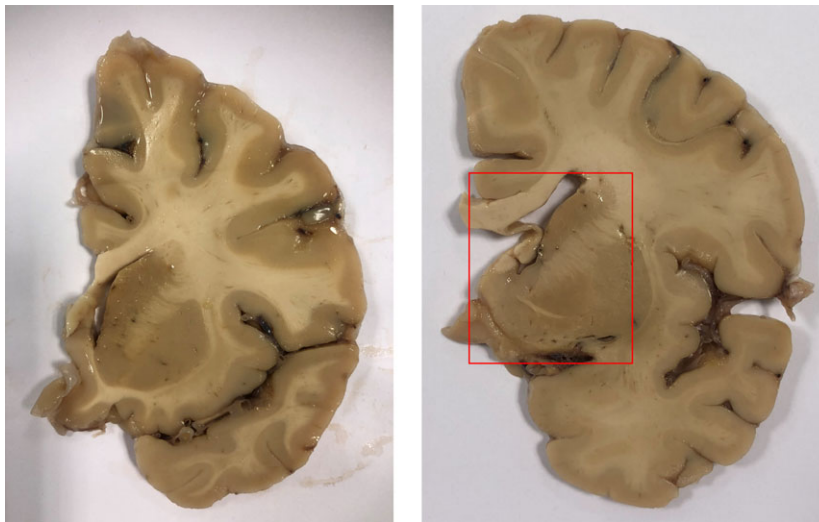


Figure 3. Photograph showing two sliced brain slabs approximately 1.0 cm (right) and 1.5 cm (left) anterior to the coronal level of the mammillary bodies. Recommended sampling for the nvIDBB is outlined by a red box at the level at or just rostral to the anterior commissure decussation. nvIDBB, nucleus of the vertical limb of the diagonal band of Broca.

absence of anterior commissure fibre), the DBB can be identified dorsal and medial to the nucleus accumbens and interposed with the midline septum pellucidum (Figure 2a–c). Moving caudally, at the ‘pre-decussation level’ (as the anterior commissure emerges laterally, but still anterior to the commissural decussation), the DBB descends ventrally but remains a compact white matter bundle situated within the ventromedial aspect of the basal forebrain (Figure 2d–f). More posteriorly, where the anterior limb of the anterior commissure becomes prominent, the DBB often splits into a much more diffuse structure, with its fibres often interspersed with streaks of grey matter (Figure 2g–i). At this level, the DBB is located lateral to a region known as the paraolfactory area [24,25] and the overall orientation of the white-matter fibres become more diagonal. Here,

the density of the ChAT-positive neurons is greatest and correlates best with the *nucleus diagonalis angularis* described by Brockhaus [21]. Finally, at the level of the anterior commissure decussation, the DBB terminates medial to the ventral striatum and the neurons are found to be orientated horizontally, parallel to the base of the forebrain (Figure 2j–l). The white-matter fibres become very diffuse and it is probably at this coronal level that Broca described the diagonal band as seen from the base of the brain [12].

Sampling strategy for the nvIDBB

Exhaustive stereotaxic analysis of the entire diagonal band may be difficult due to limited availability of human brain tissue, particularly in clinical or tissue

Table 1. Guidelines for the identification of neurons within the nucleus of the vertical limb of the diagonal band of Broca

<i>Feature</i>	<i>Description</i>
Anteroposterior level at coronal plane	Neurons can be identified at the 'pre-decussation' level (Figure 2d,g) of the anterior basal ganglia
Dendritic orientation	Neurons are orientated at an oblique angle to the ventral border of the basal forebrain. Nucleus basalis of Meynert neurons are orientated parallel to the ventral border
Visibility of diagonal band	Cells are embedded within the myelinated fibres of the diagonal band, identified on myelin counterstain or myelin-stained serial sections

bank setting. Furthermore, the heterogeneity of cell density and anatomy do not lend themselves to sampling the entire extent. Instead, we propose that sampling a dense and reliably defined part of the nvIDBB would provide a more representative and accurate representation and enable consistent sampling of this important region. Depending on brain size, the area of maximal nvIDBB density is situated approximately 10–15 mm anterior to the coronal level of the mid-mammillary body (Figure 3).

Due to the lack of clearly defined boundaries between overlapping cell groups within the basal forebrain cholinergic complex, the following guide can be used to distinguish the nvIDBB from surrounding basal forebrain nuclei (Table 1):

First, isolated nvIDBB neurons are often found at the 'pre-decussation' level (Figure 2). At the rostral-most level (typically precommissural as shown in Figure 2a), the MSN forms a continuous, vertically orientated column of magnocellular neurons with the nvIDBB embedded within the septal grey matter. However, in contrast to the nvIDBB, only approximately 10% of MSN neurons are ChAT-immunopositive. At this coronal level, previous authors have separated MSN from nvIDBB based on a rarefaction of ChAT-immunostained neuron density [6] and different neuronal morphology (with MSN neurons being generally smaller and ovoid in shape) [7]. At the level of the anterior commissure decussation, the caudoventral part of the nvIDBB is often found to be interdigitated with the medial nbM magnocellular neurons, particularly the anteromedial sector of the Ch4 (Ch4am) [8].

Second, the direction of general dendritic orientation of the neurons is important for distinguishing nvIDBB from other neuronal groups. In a detailed morphometric study using thick (240 µm) basal forebrain sections with a Golgi impregnation technique, Arendt and colleagues [27] described a gradual shift in dendritic orientation from a ventrodorsal orientation at the MSN and the rostral nvIDBB to a mediolateral orientation at the caudal nvIDBB and nbM. Neurons in the nvIDBB should be orientated at an oblique angle from the ventral border of the basal forebrain, which can be distinguished from those in the nbM which are orientated in a parallel fashion.

As suggested by various investigators, neurons in the nvIDBB are interspersed within the DBB [21,25,28], and counterstaining serial sections stained for myelin (luxol-fast blue staining) can be helpful for identifying where the neurons reside with respect to the DBB fibre tracts.

A probabilistic approach to identify neurons within the nvIDBB

Due to the overlapping arrangement of basal forebrain structures, intersubject variability may greatly affect delineation of nvIDBB from surrounding cholinergic cell groups. One approach to minimize uncertainty is to use a stereotaxic probabilistic map of brain structures, an approach popular among brain imaging scientists. This technique uses a small sample of serially and histologically stained, post-mortem brain samples mapped on to a reference brain with magnetic resonance imaging (MRI) images, creating a probabilistic map, showing the likelihood for a certain structure found to be within a reference space in brain imaging [29]. Probabilistic maps of various cortical and subcortical regions, including the basal forebrain, are presently available [29]. Zaborszky and colleagues [30] have published detailed stereotaxic probabilistic maps of the four basal forebrain cholinergic cell groups also including the often neglected posterior nbM (Ch4p) component in the mapping. However, in their study, no distinction was made between nvIDBB (Ch2) and MSN (Ch1). Furthermore, their initial delineation of the four cholinergic cell groups was largely based on Mesulam and colleagues' classification on rhesus monkeys [7], which may not reliably map well on to human brains. For future brain imaging studies focusing on the nvIDBB, a

more detailed probabilistic map separating the nvIDBB and the MSN may be required.

Distinction between the anterior (rostral) and posterior (caudal) basal forebrain compartments

Although different basal forebrain compartments appear to be continuous, there have been suggestions that they are developed from a dual embryological origin. Based on observations in rats and cats, the caudal basal forebrain (including the nbM) arises earlier than the rostral components (MSN and nvIDBB) which later merge and form a continuum (reviewed in [2]). Although it is unknown whether the same is true for humans, one could speculate that component-specific vulnerability may exist in different neurological disorders. In one recent MRI study on patients with amnesic mild cognitive impairment and controls, Cantero and colleagues reported the volume changes in the rostral basal forebrain including the MSN and nvIDBB significantly correlated with changes in hippocampal volume in both groups, whereas that of the caudal basal forebrain only significantly correlated with variations of amygdala and temporal cortical volumes. Hence, in future studies, it is important to carefully delineate these basal forebrain nuclei and perform more in-depth analysis.

What about the nucleus of the horizontal limb of the diagonal band?

Cells in the nhlIDBB can be found both amongst the fibres of the horizontal portion of the DBB and beneath the substantia innominata, parallel to the ventral surface of the basal forebrain. They are described as generally smaller than nbM neurons (10–15 μm in diameter) and are fusiform and multipolar in shape [7,31]. However, in primates, only approximately 1% of the nhlIDBB neurons are cholinergic, overlapping heavily with neurons in the nbM [7] and understandably for studies of cholinergic innervation, this nucleus is often neglected.

Revisiting the cholinergic nvIDBB in different neurological diseases

After establishing the anatomy of the nvIDBB, we carried out an extensive literature review to establish the

pattern of cell loss within the nvIDBB in several neurological disorders. Due to the difficulty in delineating boundaries, some studies grouped the MSN and nvIDBB as they share a common efferent pathway towards the hippocampal complex [4,32–36]. Furthermore, most investigators have used the terminology Ch2 when quantifying neuronal loss within nvIDBB, though this term should strictly be used on ChAT-immunostained tissue to define the local cholinergic population. Thus, in this review, we avoid using Ch terminology unless the particular study carried out quantitative assessment with a specific cholinergic marker.

The nvIDBB in AD

Quantitative studies on the nvIDBB in AD have reported conflicting results ranging from no cell loss to a maximum of 84% loss (Table 2). Loss of nvIDBB neurons was mainly reported in earlier studies using cresyl violet (Nissl stain) for the visualization of neurons, and the degree of cell loss did not appear to differ between early and late-onset AD [37]. Neuronal loss in the nvIDBB was correlated to senile plaque density in the hippocampus of AD cases by one group [4], but this correlation was not observed in another study [37]. It was later suggested that neurons within the basal forebrain cholinergic group undergo atrophy instead of cell loss in AD [34]. Indeed, when size criteria were eliminated for the quantification of neurons within the nvIDBB, no significant cell loss was observed in AD cases relative to age-matched controls. This is supported by the higher reported nvIDBB cell loss in studies only quantifying neurons larger than 30 μm in diameter (70–80% loss) [37,38] compared with those quantifying neurons larger than 20 μm in diameter (41–67.5% loss) [4,32,39,40]. Using appropriate immunohistochemistry, a size criterion to distinguish neurons from other cell types is not needed as both large and atrophied neurons will be stained, although the latter will only be positive if metabolically active and preserving a cholinergic phenotype. One study using immunohistochemistry to label nerve growth factor (NGF) receptors (NGFR), which coexpress in over 95% of the basal forebrain cholinergic neurons, failed to observe any significant neuronal loss in the nvIDBB in the seven AD cases studied [33]. This is supported by a previous finding that NGF gene expression is decreased in the nbM but not the MSN and nvIDBB of

Table 2. Studies quantifying changes of the nvDDB and MSN neurons

Year	Authors	Stains for identification of neurons	Neuronal count criteria	Disease	n	Mean age at death	%nvDDB loss from control	%MSN loss from control	%nvDDB + MSN loss from control
AD									
1983	Arendt <i>et al.</i> [39]	Nissl	>20 µm diameter, abundant Nissl substance	AD	14	60.8	67.50%	63.71%	–
1985	Arendt <i>et al.</i> [4]	Nissl	>20 µm diameter, abundant Nissl substance	AD	5	60.8	–	–	62.50%
1986	Etienne <i>et al.</i> [37]	Nissl	>30 µm diameter, visible nucleus, abundant Nissl substance	AD	9	78.9	70% (mean); 83.56% (max)	–	–
1987	Gertz <i>et al.</i> [32]	Nissl	>20 µm diameter, nucleated nerve cells	AD	7	91.1	–	–	54.20%
1988	Wilcock <i>et al.</i> [40]	Nissl	>20 µm diameter, visible nucleolus, abundant Nissl substance	AD	10	79.3	41.09% (mean); 41.42% (max)	–	–
1989	Mufson <i>et al.</i> [33]	NGFR	Immunoreactive cell soma	AD	7	77	–	–	16.7% (n.s.)
1990	Vogels <i>et al.</i> [34]	Nissl	Nissl-stained, visible nucleolus	AD	10	84.5	–	–	No loss
1993	Lehericy <i>et al.</i> [6]	ChAT	ChAT-positive cell body (displaying either strong or light immunostaining)	AD	4	89.5	56%	53%	55%
1995	Arendt <i>et al.</i> [43]	Nissl	>20 µm diameter, visible nucleus, abundant Nissl substance	AD	15	65	–	–	Approximately 78% [†] (vs. adult control); approximately 64.5% (vs. elderly control)
1995	Poirier <i>et al.</i> [38]	Nissl & AChE	AChE-positive, >30 µm, abundant Nissl substance on adjacent section	AD	8 (from 24)	Unknown for the eight selected cases	Approximately 60% [†] (ApoE4 negative); approximately 80% [†] (ApoE4 positive)	–	–
2006	Fujishiro <i>et al.</i> [35]	ChAT	ChAT-immunopositive cells	AD	4	83.5	–	–	n.s.
Lewy body disorders									
1983	Whitehouse <i>et al.</i> [42]	Nissl	>30 µm diameter, abundant Nissl substance	PD	3	60	n.s.	–	–
1983	Arendt <i>et al.</i> [39]	Nissl	>20 µm diameter, abundant Nissl substance	PDD	2	71.5	44.80%	–	–
			>20 µm diameter, abundant Nissl substance	PD	5	58.5	76.60%	69.80%	–

Table 2. (Continued)

Year	Authors	Stains for identification of neurons	Neuronal count criteria	Disease	n	Mean age at death	%nvIDBB loss from control	%MSN loss from control	%nvIDBB + MSN loss from control
1995	Arendt <i>et al.</i> [43]	Nissl	>20 µm diameter, visible nucleus, abundant Nissl substance	PD	6	58.2	–	–	Approximately 75% [†] (vs. adult control); approximately 59.7% (vs. elderly control)
2006	Fujishiro <i>et al.</i> [35]	ChAT	ChAT-immunopositive cells	DLB	8	75	–	–	Approximately 45% [†]
2014	Hall <i>et al.</i> [36]	ChAT	ChAT-immunopositive cells	PD PDD	5 6	60.4 60.2	–	–	n.s. n.s.
Other neurological diseases									
1983	Whitehouse <i>et al.</i> [42]	Nissl	>30 µm diameter, abundant Nissl substance	Post-encephalitic Parkinsonism	1	50.3	85.16% increase	–	–
1983	Arendt <i>et al.</i> [39]	Nissl	>20 µm diameter, abundant Nissl substance	Korsakoff's disease	3	43.3	56.67%	40.33%	–
1984	Arendt <i>et al.</i> [47]	Nissl	>20 µm diameter, abundant Nissl substance	CJD	1	47	–	–	43% (right hemisphere); 39% (left hemisphere)
1985	Bauman <i>et al.</i> [48]	Nissl	Visible nucleoli	Infantile autism	1	29	11% (n.s.)	54% increase	–
1995	Arendt <i>et al.</i> [43]	Nissl	>20 µm diameter, visible nucleus, abundant Nissl substance	Ageing Korsakoff's disease with Wernicke's encephalopathy	11 6	78.1 39.5	–	–	Approximately 38% [†] (vs. adult control) Approximately 68% [†] (vs. adult control); approximately 48.4% (vs. elderly control)
2013	Rüb <i>et al.</i> [50]	Nissl	All countable Nissl-stained neurons	SCA2	4	54.8	74%	72%	–

Studies using immunohistochemical markers for the identification of cholinergic neurons within the nvIDBB are shaded in grey.

AChE, acetylcholinesterase; AD, Alzheimer's disease; ChAT, choline acetyltransferase; CJD, Creutzfeldt–Jakob disease; DLB, dementia with Lewy bodies; MSN, medial septal nucleus; NGFR, nerve growth factor receptor; n.s., no significance; nvIDBB, nucleus of the vertical limb of diagonal band of Broca; PD, Parkinson's disease; PDD, PD dementia; SCA2, spinocerebellar ataxia type 2.

[†]Approximation from graphs within the study.

AD cases [41]. However, studies using ChAT immunohistochemistry on nvIDBB neurons reported contrasting results. An early study on four AD cases (mean age at death = 89.5) found 56% ChAT-positive neuronal loss in the nvIDBB and 53% loss in the MSN with no significant change in mean neuronal cross-sectional area [6], whereas a more contemporary study found neuronal shrinkage but no significant loss of Ch1/2 neurons in four AD cases (mean age at death = 83.5) [35]. One explanation for these differences could be a differing sensitivity of anti-ChAT antibodies and immunohistochemical amplification techniques. In Lehericy *et al.*'s study, primary antibodies were incubated for 3 days prior to signal amplification with peroxidase antiperoxidase technique, possibly suggesting a lower sensitivity of the primary antibody used. Therefore, it is likely that neurons with a diminished expression of ChAT, particularly in AD [34], may not be stained and quantified. Nevertheless, there is a general consensus that this rostral cholinergic basal forebrain is relatively spared in AD.

The nvIDBB in PD and Lewy body dementias

In contrast to AD, there have only been a small number of studies investigating neuronal loss in the nvIDBB in Lewy body disorders (Table 2). Whitehouse and colleagues used Nissl staining for neuronal counts and first reported 44.8% loss of nvIDBB neurons in two PD with dementia (PDD) cases but no significant change in three PD cases [42]. Subsequently, using a neuronal counting criterion to include neurons larger than 20 μm in diameter, one study with five PD cases reported 76.6% loss of nvIDBB and 69.8% MSN neurons [4] and another with six PD cases reported 59.7% loss of nvIDBB and MSN neurons [43]. Recently, with ChAT-immunohistochemistry, one study with eight dementia with Lewy bodies (DLB) cases reported significant Ch1/2 loss relative to age-matched controls and AD cases [35]. The cell loss was accompanied by a reduction of mean surface area of ChAT-positive cell bodies, an indicator of cell size. Another study using post-mortem tissues from a prospective and clinically well-characterized cohort found an increased variation in cell number but no significant ChAT-positive neuronal loss in the Ch1/2 region of five PD and six PDD cases, although a trend towards a decrease in neuron number was seen in progression from PD to PDD [36].

Both studies have linked the change in nvIDBB neuronal count in Lewy body disease cases to an increase in ubiquitin-positive, alpha-synuclein Lewy neurite pathology in the CA2 subsector of the hippocampus, as reported by previous studies [44–46], which has been associated with cognitive impairment seen in Lewy body disorders.

The nvIDBB in other neurological conditions

Degeneration of the nvIDBB is not exclusive to neurodegenerative diseases (Table 2). Indeed, an approximately 38% nvIDBB and MSN neuronal loss has been reported in aged brains (mean age at death = 78.1) when compared to younger adult controls [43]. In Korsakoff's disease, neuronal loss within the nvIDBB has been reported to be about 50% [39,43]. Single case studies on post-encephalitic Parkinsonism [42], Creutzfeldt-Jakob disease [47] and infantile autism [48] have all reported varying degrees of alteration in neuronal count/density within the nvIDBB. Interestingly, severe basal forebrain cholinergic degeneration has been reported in spinocerebellar ataxia (SCA) types 1 (SCA1) and 2 (SCA2) with relatively well-preserved cognitive function [49,50]. In particular, one study reported neuronal loss in the MSN (72% loss), nvIDBB (74% loss) and nbM (86% loss) in four SCA2 cases compared with controls without significant correlation with tau pathology according to Braak and Braak AD stage [50], indicating a possible causal role of polyglutamine expansion in the death of basal forebrain cholinergic neurons.

Consideration of the noncholinergic components in the cholinergic basal forebrain complex

As discussed previously, 90% of nbM magnocellular neurons in the primate basal forebrain express the cholinergic marker, ChAT [7]. However, the proportion of cholinergic to noncholinergic neurons is much smaller in rostral cholinergic groups (10% in MSN, 70% in nvIDBB and 1% in nhIDBB). Therefore, previous studies using Nissl staining for quantification of neurons in the MSN and nvIDBB will also be describing pathology in the noncholinergic components of the basal forebrain. The neurochemical profiles of noncholinergic rostral basal forebrain neurons have been extensively

investigated in rodents and nonhuman primates. Tyrosine-hydroxylase-positive neurons have been found in the basal forebrain [51], while γ -aminobutyric acid (GABA)-ergic [52] and glutamatergic neurons [53] form the largest noncholinergic hippocampal-projecting group within MSN/nvIDBB. In rodent studies, low frequency theta rhythm in the hippocampus is generated in the MSN-nvIDBB, mainly through GABAergic output neurons, and contributes to spatial learning and memory [54,55]. GABAergic output neurons from the MSN/nvIDBB form synaptic contacts with hippocampal interneurons and act as pacemaker cells for theta rhythm with disinhibition of hippocampal pyramidal neurons [55]. Recent studies also showed glutamatergic neurons modulate theta rhythm via local modulation of GABAergic neurons within MSN/nvIDBB [56]. Since MSN/nvIDBB neuronal loss was initially reported in AD cases with little or no significant loss in the ChAT-immunopositive component, it could be hypothesized that there may be a greater GABAergic and glutamatergic MSN/nvIDBB neuronal loss in AD.

NGF and its receptors (high affinity, trkA and low affinity, p75^{NTR}) colocalize within the human cholinergic basal forebrain [33,57,58] and reduced NGFR levels and mRNA expression were reported in the nbM, but not the nvIDBB, of AD brains [33,41]. In addition, galanin, a 19 or 30-amino acid long peptide in human brain, is coexpressed by basal forebrain cholinergic neurons. In AD and PD, galanin was shown to display a higher degree of presence ('hyperinnervation') in surviving ChAT-positive neurons, particularly in the anterior basal forebrain [59–61].

Functional correlates to the differential pattern of nvIDBB cell loss in Alzheimer's and PD

Functional connections of the nvIDBB in the human brain remain largely unknown, but case studies from specific vascular lesions have provided some clues. There are two major sources of vascular supply to the basal forebrain. The anterior/septal sector of the basal forebrain (including MSN and nvIDBB) is supplied by perforator arteries of the anterior communicating artery; the caudal/horizontal sector (including the nhIDBB and nbM) is supplied by the anterior lenticulostriate branches from the proximal (A1) sector of the anterior cerebral artery [62].

Amnesia and Korsakoff's syndrome-like symptoms have been reported in patients after repairs of ruptured anterior communicating artery aneurysm causing infarction of the anterior basal forebrain [63–71]. These lesions tend to be widespread and affect multiple basal forebrain nuclei and fibre tracts. Nevertheless, two studies reported cases with relatively discrete basal forebrain lesions [72,73]. In one of the cases reported by Damasio and colleagues, surgical clipping of an aneurysm at the A1 and A2 junction of the left anterior cerebral artery was performed [72]. The anatomical regions affected by this lesion were similar to a case reported by Abe and colleagues showing an isolated lesion at the right nvIDBB, anterior hypothalamus and lamina terminalis [73]. Hypoperfusion caused by the lesion extended to both sides of the hemisphere as shown by single-photon emission computed tomography scan using ^{99m}Tc-d, l-hexamethyl propyleneamine oxime. In both cases, neuropsychiatric tests were performed and the patients exhibited anterograde and retrograde amnesia. However, there was a benefit with cueing that indicated a deficit in retrieval rather than encoding of memory. A similar amnesic profile was reported by Morris and colleagues on a case with surgical resection of a low-grade astrocytoma at the right anterior basal ganglia region containing the nvIDBB [74]. From these three cases, it is evident that the nvIDBB is involved in memory function and in particular memory retrieval.

According to the Movement Disorder Society Task Force consensus criteria on the diagnosis of PDD, patients with PDD may suffer impairment in free recall which improves with cueing [75]. There is a general agreement that memory impairment in PD involves deficit in memory retrieval rather than storage/encoding memory as in AD [75]. Therefore, it can be deduced that nvIDBB may be more significantly affected in Lewy body disorders than in AD. This is supported by an aforementioned post-mortem study by Fujishiro and colleagues reporting a significant decrease in ChAT-positive neurons in the nvIDBB of DLB cases relative to AD and age-matched controls [35]. However, a recent imaging study with 11 AD and 11 DLB patients failed to demonstrate difference in MSN/nvIDBB atrophy on structural MRI scans [76]. Instead, only a trend reduction in MSN/nvIDBB volume was observed in AD (−17.5%) and DLB (−17.4%). This discrepancy may be due to the fact that *in vivo* MRI-based measurement

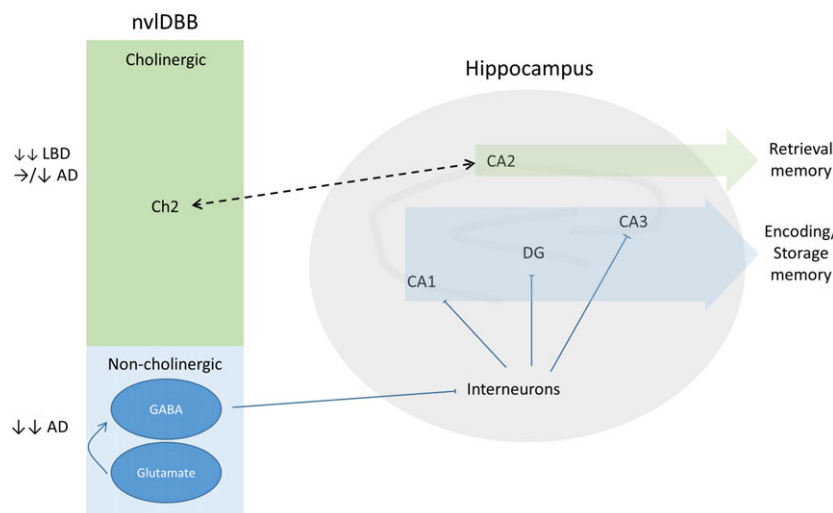


Figure 4. Proposed schema for the neurodegenerative changes within cholinergic and noncholinergic populations of the nvIDBB in Lewy body disorders and AD with possible clinicopathological correlates. AD, Alzheimer's disease; CA, Cornu Ammonis; Ch2, cholinergic population of the vertical limb of the diagonal band of Broca; DG, dentate gyrus; GABA, γ -aminobutyric acid; LBD, Lewy body disorder; nvIDBB, nucleus of the vertical limb of the DBB.

cannot distinguish whether neuronal loss or cell atrophy contributes to the volumetric changes. Thus, further post-mortem studies will be required.

Ch2 and CA2: a possible connection?

Similar to the nvIDBB, the hippocampal CA2 subfield is a relatively unexplored region in the human brain. Recently, using retrograde and adeno-associated virus-expressing anterograde tracers, reciprocal connections between the MSN-nvIDBB and the CA2 have been identified in the mouse brain [77]. Ubiquitin- and alpha-synuclein-immunopositive neuritic pathology in Lewy body disorders has been found confined to the CA2 subfield in the hippocampus [36,44–46], in contrast to the preferential deposition of neurofibrillary tangles in the CA1 region in AD [78]. Coincidentally, this is the subregion where the highest density of ChAT-positive fibres and punctate immunoprecipitates can be identified in the human hippocampus [79]. Although the presence of hippocampal dopaminergic innervation has been extensively reported in rodents [80], evidence of such projection in the human brain was lacking with one study failing to demonstrate the presence of monoaminergic fibre in the hippocampus of DLB and aged control brains using immunostaining with antityrosine hydroxylase antibodies [45]. Significant hippocampal cholinergic depletion was found in PDD cases

when compared with PD and control [36]. The subfield-specific protein aggregation pathology and cholinergic deficits in the hippocampus of Lewy body disorders appeared to be associated with the severe nvIDBB cholinergic depletion described in the sections above. As a result, it can be hypothesized that Lewy pathologies in the CA2 subregion of the hippocampus can cause neurodegeneration of the cholinergic component of the nvIDBB (Ch2) leading to deficits in retrieval memory, while a predominant noncholinergic neuronal loss of the nvIDBB may contribute to the encoding and storage memory deficits in AD (Figure 4).

Conclusion

The functional importance of the diagonal band in human cognition has long been recognized owing to its anatomical position in the limbic loop. However, the pathological significance of the nucleus of the diagonal band, particularly the nvIDBB, in neurodegenerative conditions has not been studied in detail. There has been a lack of consensus quantifying cholinergic cell loss in AD and Lewy body disorders primarily due to the following: (i) the absence of clear anatomical boundaries to delineate nvIDBB from surrounding magnocellular basal forebrain nuclei; (ii) application of size criteria for neuronal quantification discounting the possibility of cell shrinkage; and (iii) most studies

attributing magnocellular neuronal loss in the nvIDBB to cholinergic nerve cells without use of a cholinergic immunohistochemical marker. Thus, by reviewing the history of DBB anatomy, we have established recommended sampling criteria for identifying the nvIDBB suitable for future clinicopathological studies. In addition, we recommend the use of specific cholinergic immunohistochemical markers such as ChAT for the identification and quantification of Ch2 (cholinergic component of nvIDBB) neurons. Further studies investigating the changes in the noncholinergic components of the nvIDBB, such as GABAergic neurons and glutamatergic interneurons, will also be needed.

Through the study of cases with discrete vascular or other lesions affecting the rostral basal forebrain, it can be deduced that the nvIDBB plays a discrete role in retrieval memory function, severely affected in Lewy body disorders. Extrapolating from existing clinicopathological studies, we propose an anatomical and functional connection between Ch2 and the CA2 subfield in the hippocampus which may be especially vulnerable to Lewy pathologies. Further clinicopathological investigations are now needed to test this hypothesis. With the development of novel tissue clearing techniques which have successfully been applied to post-mortem human brain tissues for the visualization of anatomical structures and their connections in three dimensions [81–83], the detailed projection of cholinergic fibres from the nvIDBB in the human brain may be mapped out, shedding more light on the detailed role of the cholinergic nvIDBB in cognitive function.

Acknowledgement

The authors thank Parkinson's UK, registered charity 258197, for their continued support as well as the donors and family for their invaluable donation of brain tissue to the Parkinson's UK Tissue Bank. The work in the Laboratory of Neurodegenerative Diseases is supported by HKU Alzheimer's Disease Research Network under Strategic Research Theme of Healthy Aging to RCCC. This work in the neuropathology unit was supported in part by NIA AG12411.

Author contributions

A. K. L. L. and E. J. L. conceived the study and wrote the first draft of the manuscript. A. K. L. L., E. J. L., I.

A. and S. M. G. collected and processed human brain materials for this study. R. C. C. C., R. K. B. P. and S. M. G. provided expertise and participated in the design of the experiments. All authors read, reviewed and edited the final manuscript.

Conflict of interest

The Editors of *Neuropathology and Applied Neurobiology* are committed to peer-review integrity and upholding the highest standards of review. As such, this article was peer-reviewed by independent, anonymous expert referees and the authors had no role in either the editorial decision or the handling of the paper.

References

- 1 Mesulam M-M. Cholinergic circuitry of the human nucleus basalis and its fate in Alzheimer's disease. *J Comp Neurol* 2013; **521**: 4124–44
- 2 Semba K. Phylogenetic and ontogenetic aspects of the basal forebrain cholinergic neurons and their innervation of the cerebral cortex. *Prog Brain Res* 2004; **145**: 3–43
- 3 Bartus RT, Dean RL, Beer B, Lippa A. The cholinergic hypothesis of geriatric memory dysfunction. *Science* 1982; **217**: 408–14
- 4 Arendt T, Bigl V, Tennstedt A, Arendt A. Neuronal loss in different parts of the nucleus basalis is related to neuritic plaque formation in cortical target areas in Alzheimer's disease. *Neuroscience* 1985; **14**: 1–14
- 5 McGeer PL, McGeer EG, Suzuki J, Dolman CE, Nagai T. Aging, Alzheimer's disease, and the cholinergic system of the basal forebrain. *Neurology* 1984; **34**: 741–5
- 6 Lehericy S, Hirsch EC, Cervera-Piérot P, Hersh LB, Bakchine S, Piette F, Duyckaerts C, Hauw JJ, Javoy-Agid F, Agid Y. Heterogeneity and selectivity of the degeneration of cholinergic neurons in the basal forebrain of patients with Alzheimer's disease. *J Comp Neurol* 1993; **330**: 15–31
- 7 Mesulam MM, Mufson EJ, Levey AI, Wainer BH. Cholinergic innervation of cortex by the basal forebrain: cytochemistry and cortical connections of the septal area, diagonal band nuclei, nucleus basalis (substantia innominata), and hypothalamus in the rhesus monkey. *J Comp Neurol* 1983; **214**: 170–97
- 8 Mesulam MM, Geula C. Nucleus basalis (Ch4) and cortical cholinergic innervation in the human brain: observations based on the distribution of acetylcholinesterase and choline acetyltransferase. *J Comp Neurol* 1988; **275**: 216–40
- 9 Liu AKL, Chang RC-C, Pearce RKB, Gentleman SM. Nucleus basalis of Meynert revisited: anatomy, history and differential involvement in Alzheimer's and Parkinson's disease. *Acta Neuropathol* 2015; **129**: 527–40

- 10 Broca P. *Mémoires d'anthropologie*. Paris: Reinwald, 1877
- 11 Broca P. Anatomie comparee des circonvolutions cerebrales: Le grand lobe limbique et la scissure limbique dans la serie des mammiferes. *Rev Anthropol* 1978; **1**: 385–498
- 12 Broca P, Pozzi S. *Mémoires sur le cerveau de l'homme et des primates*. Paris: C. Reinwald, 1888
- 13 Swanson L. *Neuroanatomical Terminology: A Lexicon of Classical Origins and Historical Foundations*. Oxford: Oxford University Press, 2014
- 14 Smith GE. The relation of the fornix to the margin of the cerebral cortex. *J Anat Physiol* 1897; **32**(Pt 1): 23–58
- 15 Johnston JB. The cell masses in the forebrain of the turtle, *Cistudo carolina*. *J Comp Neurol* 1915; **25**: 393–468
- 16 Crosby EC. The forebrain of Alligator mississippiensis. *J Comp Neurol* 1917; **27**: 325–402
- 17 Johnston JB. Further contributions to the study of the evolution of the forebrain. *J Comp Neurol* 1923; **35**: 337–481
- 18 Gray PA. The cortical lamination pattern of the opossum, *Didelphys virginiana*. *J Comp Neurol* 1924; **37**: 221–63
- 19 Gurdjian ES. The corpus striatum of the rat. Studies on the brain of the rat. No. 3. *J Comp Neurol* 1928; **45**: 249–81
- 20 Papez JW, Aronson LR. Thalamic nuclei of pithecus (macacus) rhesus. *Arch Neurol Psychiatry* 1934; **32**: 1–26
- 21 Brockhaus H. Vergleichend-anatomische Untersuchungen über den Basalkernkomplex. *J Psychol Neurol* 1942; **51**: 57–95
- 22 Andy OJ, Stephan H. The septum in the human brain. *J Comp Neurol* 1968; **133**: 383–410
- 23 Daitz HM, Powell TP. Studies of the connexions of the fornix system. *J Neurol Neurosurg Psychiatry* 1954; **17**: 75–82
- 24 Schaltenbrand G, Bailey P. *Einführung in die Stereotaktischen Operationen Mit Einem Atlas des Menschlichen Gehirns* [Introduction to Stereotaxis with an Atlas of the Human Brain], Vol. 1–3. Stuttgart: Georg Thieme Verlag, 1959
- 25 Nieuwenhuys R, Voogd J, Van Huijzen C. *The Human Central Nervous System: A Synopsis and Atlas*. Berlin: Springer Science & Business Media, 2007
- 26 Mai JK, Majtanik M, Paxinos G. *Atlas of the Human Brain*. San Diego: Academic Press, 2016
- 27 Arendt T, Marcova L, Bigl V, Brückner MK. Dendritic reorganisation in the basal forebrain under degenerative conditions and its defects in Alzheimer's disease. I. Dendritic organisation of the normal human basal forebrain. *J Comp Neurol* 1995; **351**: 169–88
- 28 Emmers R, Akert K. *A Stereotaxic Atlas of the Brain of the Squirrel Monkey Saimiri Sciureus; Emmers, Raimond, and Konrad Akert; With a Forew. by Clinton N. Woolsey*. Bethesda: University of Wisconsin Press, 1963
- 29 Amunts K, Zilles K. Architectonic mapping of the human brain beyond brodmann. *Neuron* 2015; **88**: 1086–107
- 30 Zaborszky L, Hoemke L, Mohlberg H, Schleicher A, Amunts K, Zilles K. Stereotaxic probabilistic maps of the magnocellular cell groups in human basal forebrain. *NeuroImage* 2008; **42**: 1127–41
- 31 Saper CB, Chelimsky TC. A cytoarchitectonic and histochemical study of nucleus basalis and associated cell groups in the normal human brain. *Neuroscience* 1984; **13**: 1023–37
- 32 Gertz HJ, Cervos-Navarro J, Ewald V. The septo-hippocampal pathway in patients suffering from senile dementia of Alzheimer's type. Evidence for neuronal plasticity? *Neurosci Lett* 1987; **76**: 228–32
- 33 Mufson EJ, Bothwell M, Kordower JH. Loss of nerve growth factor receptor-containing neurons in Alzheimer's disease: a quantitative analysis across subregions of the basal forebrain. *Exp Neurol* 1989; **105**: 221–32
- 34 Vogels OJ, Broere CA, ter Laak HJ, ten Donkelaar HJ, Nieuwenhuys R, Schulte BP. Cell loss and shrinkage in the nucleus basalis Meynert complex in Alzheimer's disease. *Neurobiol Aging* 1990; **11**: 3–13
- 35 Fujishiro H, Umegaki H, Isojima D, Akatsu H, Iguchi A, Kosaka K. Depletion of cholinergic neurons in the nucleus of the medial septum and the vertical limb of the diagonal band in dementia with Lewy bodies. *Acta Neuropathol* 2006; **111**: 109–14
- 36 Hall H, Reyes S, Landeck N, Bye C, Leanza G, Double K, Thompson L, Halliday G, Kirik D. Hippocampal Lewy pathology and cholinergic dysfunction are associated with dementia in Parkinson's disease. *Brain* 2014; **137**: 2493–508
- 37 Etienne P, Robitaille Y, Wood P, Gauthier S, Nair NP, Quirion R. Nucleus basalis neuronal loss, neuritic plaques and choline acetyltransferase activity in advanced Alzheimer's disease. *Neuroscience* 1986; **19**: 1279–91
- 38 Poirier J, Delisle MC, Quirion R, Aubert I, Farlow M, Lahiri D, Hui S, Bertrand P, Nalbantoglu J, Gilfix BM, Gauthier S. Apolipoprotein E4 allele as a predictor of cholinergic deficits and treatment outcome in Alzheimer disease. *Proc Natl Acad Sci USA* 1995; **92**: 12260–4
- 39 Arendt T, Bigl V, Arendt A, Tennstedt A. Loss of neurons in the nucleus basalis of Meynert in Alzheimer's disease, paralysis agitans and Korsakoff's disease. *Acta Neuropathol* 1983; **61**: 101–8
- 40 Wilcock GK, Esiri MM, Bowen DM, Hughes AO. The differential involvement of subcortical nuclei in senile dementia of Alzheimer's type. *J Neurol Neurosurg Psychiatry* 1988; **51**: 842–9
- 41 Higgins GA, Mufson EJ. NGF receptor gene expression is decreased in the nucleus basalis in Alzheimer's disease. *Exp Neurol* 1989; **106**: 222–36

- 42 Whitehouse PJ, Hedreen JC, White CL, Price DL. Basal forebrain neurons in the dementia of Parkinson disease. *Ann Neurol* 1983; **13**: 243–8
- 43 Arendt T, Brückner MK, Bigl V, Marcova L. Dendritic reorganisation in the basal forebrain under degenerative conditions and its defects in Alzheimer's disease. II. Ageing, Korsakoff's disease, Parkinson's disease, and Alzheimer's disease. *J Comp Neurol* 1995; **351**: 189–222
- 44 Dickson DW, Ruan D, Crystal H, Mark MH, Davies P, Kress Y, Yen SH. Hippocampal degeneration differentiates diffuse Lewy body disease (DLBD) from Alzheimer's disease: light and electron microscopic immunocytochemistry of CA2-3 neurites specific to DLBD. *Neurology* 1991; **41**: 1402–9
- 45 Dickson DW, Schmidt ML, Lee VM, Zhao ML, Yen SH, Trojanowski JQ. Immunoreactivity profile of hippocampal CA2/3 neurites in diffuse Lewy body disease. *Acta Neuropathol* 1994; **87**: 269–76
- 46 Irwin DJ, White MT, Toledo JB, Xie SX, Robinson JL, Van Deerlin V, Lee VM-Y, Leverenz JB, Montine TJ, Duda JE, Hurtig HI, Trojanowski JQ. Neuropathologic substrates of Parkinson disease dementia. *Ann Neurol* 2012; **72**: 587–98
- 47 Arendt T, Bigl V, Arendt A. Neurone loss in the nucleus basalis of Meynert in Creutzfeldt-Jakob disease. *Acta Neuropathol* 1984; **65**: 85–8
- 48 Bauman M, Kemper TL. Histoanatomic observations of the brain in early infantile autism. *Neurology* 1985; **35**: 866
- 49 Rüb U, Bürk K, Timmann D, den Dunnen W, Seidel K, Farrag K, Brunt E, Heinsen H, Egensperger R, Bornemann A, Schwarzacher S, Korf HW, Schöls L, Bohl J, Dellerr T. Spinocerebellar ataxia type 1 (SCA1): new pathoanatomical and clinico-pathological insights. *Neuropathol Appl Neurobiol* 2012; **38**: 665–80
- 50 Rüb U, Farrag K, Seidel K, Brunt ER, Heinsen H, Bürk K, Melegh B, von Gall C, Auburger G, Bohl J, Korf HW, Hoche F, den Dunnen W. Involvement of the cholinergic basal forebrain nuclei in spinocerebellar ataxia type 2 (SCA2). *Neuropathol Appl Neurobiol* 2013; **39**: 634–43
- 51 Gouras GK, Rance NE, Scott Young W, Koliatsos VE. Tyrosine-hydroxylase-containing neurons in the primate basal forebrain magnocellular complex. *Brain Res* 1992; **584**: 287–93
- 52 Walker LC, Price DL, Young WS. GABAergic neurons in the primate basal forebrain magnocellular complex. *Brain Res* 1989; **499**: 188–92
- 53 Colom LV, Castaneda MT, Reyna T, Hernandez S, Garrido-Sanabria E. Characterization of medial septal glutamatergic neurons and their projection to the hippocampus. *Synapse* 2005; **58**: 151–64
- 54 Colgin LL. Rhythms of the hippocampal network. *Nat Rev Neurosci* 2016; **17**: 239–49
- 55 Freund TF, Antal M. GABA-containing neurons in the septum control inhibitory interneurons in the hippocampus. *Nature* 1988; **336**: 170–3
- 56 Robinson J, Manseau F, Ducharme G, Amilhon B, Vigneault E, El Mestikawy S, Williams S. Optogenetic activation of septal glutamatergic neurons drive hippocampal theta rhythms. *J Neurosci* 2016; **36**: 3016–23
- 57 Hefti F, Mash DC. Localization of nerve growth factor receptors in the normal human brain and in Alzheimer's disease. *Neurobiol Aging* 1989; **10**: 75–87
- 58 Kordower JH, Gash DM, Bothwell M, Hersh L, Mufson EJ. Nerve growth factor receptor and choline acetyltransferase remain colocalized in the nucleus basalis (Ch4) of Alzheimer's patients. *Neurobiol Aging* 1989; **10**: 67–74
- 59 Chan-Palay V. Galanin hyperinnervates surviving neurons of the human basal nucleus of Meynert in dementias of Alzheimer's and Parkinson's disease: a hypothesis for the role of galanin in accentuating cholinergic dysfunction in dementia. *J Comp Neurol* 1988; **273**: 543–57
- 60 Mufson EJ, Cochran E, Benzing W, Kordower JH. Galaninergic innervation of the cholinergic vertical limb of the diagonal band (Ch2) and bed nucleus of the stria terminalis in aging. *Dement Geriatr Cogn Dis* 1993; **4**: 237–50
- 61 Alexandris A, Liu AKL, Chang RC-C, Pearce RKB, Gentleman SM. Differential expression of galanin in the cholinergic basal forebrain of patients with Lewy body disorders. *Acta Neuropathol Commun* 2015; **3**: 77
- 62 Román GC, Kalaria RN. Vascular determinants of cholinergic deficits in Alzheimer disease and vascular dementia. *Neurobiol Aging* 2006; **27**: 1769–85
- 63 Talland GA, Sweet WH, Ballantine HT. Amnesic syndrome with anterior communicating artery aneurysm. *J Nerv Ment Dis* 1967; **145**: 179–92
- 64 Logue V, Durward M, Pratt RT, Piercy M, Nixon WL. The quality of survival after rupture of an anterior cerebral aneurysm. *Br J Psychiatry* 1968; **114**: 137–60
- 65 Gade A. Amnesia after operations on aneurysms of the anterior communicating artery. *Surg Neurol* 1982; **18**: 46–9
- 66 Volpe BT, Hirst W. Amnesia following the rupture and repair of an anterior communicating artery aneurysm. *J Neurol Neurosurg Psychiatry* 1983; **46**: 704–9
- 67 Alexander MP, Freedman M. Amnesia after anterior communicating artery aneurysm rupture. *Neurology* 1984; **34**: 752
- 68 Parkin AJ, Leng NRC, Stanhope N, Smith AP. Memory impairment following ruptured aneurysm of the anterior communicating artery. *Brain Cogn* 1988; **7**: 231–43
- 69 Phillips S, Sangalang V, Sterns G. Basal forebrain infarction. A clinicopathologic correlation. *Arch Neurol* 1987; **44**: 1134–8
- 70 Vilkki J. Amnesic syndromes after surgery of anterior communicating artery aneurysms. *Cortex* 1985; **21**: 431–44

- 71 Lindqvist G, Norlén G. Korsakoff's syndrome after operation on ruptured aneurysm of the anterior communicating artery. *Acta Psychiatr Scand* 1966; **42**: 24–34
- 72 Damasio AR, Graff-Radford NR, Eslinger PJ, Damasio H, Kassel N. Amnesia following basal forebrain lesions. *Arch Neurol* 1985; **42**: 263–71
- 73 Abe K, Inokawa M, Kashiwagi A, Yanagihara T. Amnesia after a discrete basal forebrain lesion. *J Neurol Neurosurg Psychiatry* 1998; **65**: 126–30
- 74 Morris MK, Bowers D, Chatterjee A, Heilman KM. Amnesia following a discrete basal forebrain lesion. *Brain* 1992; **115**(Pt 6): 1827–47
- 75 Emre M, Aarsland D, Brown R, Burn DJ, Duyckaerts C, Mizuno Y, Broe GA, Cummings J, Dickson DW, Gauthier S, Goldman J, Goetz C, Korczyn A, Lees A, Levy R, Litvan I, McKeith I, Olanow W, Poewe W, Quinn N, Sampaio C, Tolosa E, Dubois B. Clinical diagnostic criteria for dementia associated with Parkinson's disease. *Mov Disord* 2007; **22**: 1689–707
- 76 Grothe MJ, Schuster C, Bauer F, Heinsen H, Prudlo J, Teipel SJ. Atrophy of the cholinergic basal forebrain in dementia with Lewy bodies and Alzheimer's disease dementia. *J Neurol* 2014; **261**: 1939–48
- 77 Cui Z, Gerfen CR, Young WS. Hypothalamic and other connections with dorsal CA2 area of the mouse hippocampus. *J Comp Neurol* 2013; **521**: 1844–66
- 78 Hyman B, Van Hoesen G, Damasio A, Barnes C. Alzheimer's disease: cell-specific pathology isolates the hippocampal formation. *Science* 1984; **225**: 1168–70
- 79 Ransmayr G, Cervera P, Hirsch E, Ruberg M, Hersh LB, Duyckaerts C, Hauw J-J, Delumeau C, Agid Y. Choline acetyltransferase-like immunoreactivity in the hippocampal formation of control subjects and patients with Alzheimer's disease. *Neuroscience* 1989; **32**: 701–14
- 80 Milner TA, Bacon CE. Ultrastructural localization of tyrosine hydroxylase-like immunoreactivity in the rat hippocampal formation. *J Comp Neurol* 1989; **281**: 479–95
- 81 Chung K, Wallace J, Kim S-Y, Kalyanasundaram S, Andalman AS, Davidson TJ, Mirzabekov JJ, Zalocusky KA, Mattis J, Denisin AK, Pak S, Bernstein H, Ramakrishnan C, Grosenick L, Gradinaru V, Deisseroth K. Structural and molecular interrogation of intact biological systems. *Nature* 2013; **497**: 332–7
- 82 Ando K, Laborde Q, Lazar A, Godefroy D, Youssef I, Amar M, Pooler A, Potier M-C, Delatour B, Duyckaerts C. Inside Alzheimer brain with CLARITY: senile plaques, neurofibrillary tangles and axons in 3-D. *Acta Neuropathol* 2014; **405**: 457–9
- 83 Liu AKL, Hurry ME, Ng OT-W, DeFelice J, Lai HM, Pearce RK, Wong GT-C, Chang RC-C, Gentleman SM. Bringing CLARITY to the human brain: visualisation of Lewy pathology in three-dimensions. *Neuropathol Appl Neurobiol* 2016; **42**: 573–87

Received 29 April 2018

Accepted after revision 6 July 2018

Published online Article Accepted on 18 July 2018